Supplementary Information

A constant-current generator by water droplets driving Schottky diode without rectifying circuit

Yahui Li,[‡ab] Qi Zhang,[‡ab] Yuhong Cao,[‡cd] Zhipeng Kang,[ab] Han Ren,[ab] Zhiyuan Hu,[ab] Mang Gao,[e] Xiaole Ma,[ab] Jinyuan Yao,[a] Yan Wang,[a] Congchun Zhang,[a] Guifu Ding,[a] Junshan Liu,[f] Jiming Bao,*[g] Hui Wang*[cd] and Zhuoqing Yang*[a]

Experimental Section

Materials

The single <100> Si wafers used in the whole experiment were 3 inches with the thickness of 525 ± 25 μm (Kaihua Jinghong Electronics Co., Ltd, Zhejiang Lijing Silicon materials Co., Ltd.). The resistivity of p-Si and n-Si used routinely in this experiment is 1-10 Ω·cm without additional instructions. AZ 4620 photoresist, AZ 400K developer were purchased from Merck Electronic Materials (Suzhou) Co., Ltd, and the developer was diluted with deionized water in a volume ratio of 1:3 before using. The platinum target (99.99%), silver target (99.99%), copper target (99.99%), chromium target (99.99%) for magnetron sputtering were purchased from Zhongnuo Advanced Material (Beijing) Technology Co., Ltd. Hydrofluoric acid (HF, ≥40%) was purchased from Shanghai Lingfeng Chemical Reagent Co., Ltd, and was diluted to 5% content before using. Acetone (General-reagent, AR, ≥99.5%) and anhydrous ethanol (General-reagent, AR, ≥99.7%) were purchased from Shanghai Titan Technology Co., Ltd, and were used directly as received.

Fabrication of metal-semiconductor-metal (MSM)

The fabrication of MSM device was involved in MEMS processing technology, as shown in Figure S21a. Firstly, AZ6420 photoresist was spin-coated on the polished Si wafer (see Table S1 for the spin coating parameters), and completed the curing in a drying oven (see Figure S21b for the detailed curing process). Then, the patterning of top electrode was conducted by ultra-violet contact exposure and development, the light intensity, exposure time, and development time were 8 mW/cm^2, 50 s, and about 200 s, respectively. To form an acceptable metal-semiconductor contact, the exposed pattern was soaked in HF solution for 30 s to remove the silicon oxides. Subsequently, the top electrode was deposited onto Si surface by magnetron sputtering. After that, the sample was placed in acetone to perform a lift-off process, and

completed the front side fabrication. Finally, the device was turned over, the bottom electrode was sputtered on the backside.

To investigate the influence of electrodes on the electrical characteristics and electricity generation of MSMs. p-Si (1-10 Ω·cm) was selected for fabricating MSM, the geometry and materials of electrode were also studied. To investigate the influence of different semiconductors on the metal-semiconductor contacts, as well as the electrical characteristics and electricity generation of the fabricated MSMs. P-Si and n-Si with different resistivities were used for fabricating MSMs based on the same electrode materials and structures, where the top and bottom electrodes were Pt, and the width of top electrode was 2 mm.

LSM characterization

LSM measurement was performed on a VK-X3000 laser scanning microscope (Keyence, Japan) under atmosphere. The top electrode was uniformly deposited on Si substrate and was fabricated over a large area (5× magnification), and the electrode width was 2 mm (Figure S21c).

AFM characterization

AFM measurements were performed on a FastScan Bio atomic force microscope (Bruker, Germany) with tapping mode, and the used probe was Ti/Pt coated Si (OMCL-AC240TS). The boundary between top electrode and Si substrate is clear with a significant height difference, where the thickness of Pt and Ag electrode is 116 nm and 366 nm (Figure S22a,d). The surfaces of Si substrate and sputtering electrodes are flat, and their average roughness is 1.54 nm, 0.48 nm, 4.16 nm, 4.76 nm for p-Si, n-Si, Pt, and Ag, respectively (Figure S22b,c,e,f). To investigate the electronegativity of Si, Kelvin probe force microscope (KPFM) mode was used to measure the contact potential difference (CPD), which is calculated as the following:

$$V_{CPD} = V_{Tip} - V_{Sample}$$

Where the V_{CPD} is the measured potential, V_{Tip} is the surface potential of probe and V_{Sample} is the surface potential of sample.

Contact angle measurement

Wettability measurements were performed on a contact angle meter with 5 μL deionized water as calibration droplet (DSA100, Germany). The static contact angles for polished p-Si, polished n-Si, Pt, and Ag are 66.2°, 59.2°, 66.7°, and 65.7°, respectively (Figure S23). Although the static contact angle of solid surfaces are less than 90°, and do not exhibit excellent hydrophobic performance. The impinging water droplet could flow away smoothly when the solid surface keep a certain inclination angle (45°).

Dynamic observation of water droplet

The dynamic behaviors of water droplet impinged onto solid surface were captured by a VEO710 high-speed camera at a typical recording speed of 20,000 frames per second (VEO710, USA). Under the case driven by a water droplet, the droplet could flow away the solid surface smoothly (Si) without much residue. Besides, five relative positions between the impinging water droplet and top electrode were also captured.

I-V measurement

Current-voltage (I-V) measurements were performed on a Keysight B2902A precision source/measure unit (SMU). The data was recorded by a Quick IV measurement software. We set the sweep function for applying source voltage, the start and stop voltage were ranged from -3 V to 3 V. In this works, the I-V characteristics of three modes were tested, such as MSM device (Figure S24a, mode 1), junctions established at the interface between sputtering electrode (top or bottom) and Si (Figure S24b,c, mode 2,3). In mode 2 and 3, the junction 2 between metal probe and Si was treated as a Schottky contact. Since the smaller the contact area, the thicker the barrier width, therefore the junction 2 usually dominates the I-V characteristics in mode 2 and 3.

Schottky-Mott measurement

Electrochemical impedance spectroscopy (EIS) was performed on a CorrTest CS350H electrochemical workstation with the potential scan mode, the data was recorded by an Ivim Software, and the plot type of Schottky-Mott was selected for analysis. The start and end scanning voltage were -1 V and 2 V, the working frequency was fixed at 10 kHz, the scanning step was 20 mV, and the equilibration time was 2 s. The values of built-in potential were calculated by linearly fitting the C-V curves.

Water-driven output measurement

The water droplets used in this experiment were obtained from a laboratory deionized water system (pH value was about 7). Water droplets were produced by a kcp-c peristaltic pump (Kamoer, China), the flowing rate was controlled at 0.22 mL/s, the impinged droplet height was 8 cm, the inclination angle of MSM was 45°, and the volume of droplet was ≈73 μL. The short-circuit current was performed through a Keithley 6514 electrometer, as seen in Figure S25. Additionally, varying the impinged position and pH values of water droplet also cause a significant difference on the output of MSM device.

UV light-driven output measurement

To better understand the output mechanism of MSM driven by water droplet, the electrical signal of MSM driven by traditional light was compared. The used light source was ultraviolet band (365 nm wavelength), and the excitation intensity was examined by an ultra-violet irradiation meter. The electrical connection of measurement was the same as that of the water-driven.

Faraday pail measurement

Faraday pail measurement was used to determine the electron gain or loss ability of different materials. The testing device was composed of a droplet generation device, Faraday cup (made of Cu foil), insulating mat, and a 6514 electrometer for recording transferred charges. Owing to the well-known strong electron-obtaining capability of FEP film, it was used as a calibration to evaluate the accuracy of the measurement. During measurement, water droplet impinges onto different solid surfaces, then the charged droplet is flew into the Faraday cup with excellent conductivity, and the changes of transferred charges are also recorded by a 6514 electrometer using the charge measurement mode.

Supporting Tables

Supporting Table S1. Spin coating parameters for AZ4620

Items	Parameter	Items	Parameter
Substrate	Single crystalline Si	**Photoresist model**	AZ 4620
Pre-spin speed	500 rpm/s	**Formal spin speed**	1500 rpm/s
Pre-spin time	10 s	**Formal spin time**	30 s
Pre-spin acceleration	500 rpm/min/s	**Formal spin acceleration**	500 rpm/min/s

Supporting Table S2. Comparison of the direct current water droplet-based electricity generators

References	Materials	Water droplet	Transferred charges (nC)	Short-circuit current (μA)	Internal resistance (Ω)	Auxiliary unit	Constant-current output
[1] **Energ. Environ. Sci. 2023**, 16(3), 1071-1081	Negatively charged PTFE	Single droplet	/	0.8-pulsed	High (>1 M)	Not required	N/A
		Multiple droplets accumulation	132	60-pulsed	High (>1 M)	Charge collection device & Gas discharge tube	N/A
[2] **ACS Nano**, **2016**, 10(8): 7297-7302.	Graphene & charged PTFE	Single droplet	/	5-pulsed	High (50 M)	Not required	N/A
[3] **Nano Energy**, **2020**, 76: 105070.	n-type Si	Single droplet	/	0.3-pulsed	High (>1 M)	Not required	N/A
[4] **Nano Energy**, **2021**, 83: 105810.	n-type Si	Single droplet	/	0.3-pulsed	High (>1 M)	Not required	N/A
[5] **Research**, 2021, 2021.	n-type & p-type Si	Single droplet	/	0.64-pulsed	High (390 k)	Not required	N/A
		Multiple droplets	/	/			Constant output
This work	p-type Si	Single droplet	>690	428.9-pulsed	Low & adjustable (0.1-10 k)	Not required	N/A
	p-type Si	Multiple droplets	/	120-constant		Not required	Constant output

Note: The research on direct current droplet-based electricity generation has only received attention in recent years, especially when it comes to semiconductor material systems. Due to the different experimental parameters of the previously reported works, we selected the highest performance described in the article for comparison. It is worth noting that the short-circuit current in the table refers to the instantaneous peak short-circuit current.

References:

[1] Dong J, Zhu L, Guo P, et al. A bio-inspired total current nanogenerator[J]. **Energy & Environmental Science**, 2023, 16(3): 1071-1081.

[2] Kwak S S, Lin S, Lee J H, et al. Triboelectrification-induced large electric power generation

from a single moving droplet on graphene/polytetrafluoroethylene[J]. **ACS Nano**, 2016, 10(8): 7297-7302.

[3] Lin S, Chen X, Wang Z L. The tribovoltaic effect and electron transfer at a liquid-semiconductor interface[J]. **Nano Energy**, 2020, 76: 105070.

[4] Zheng M, Lin S, Tang Z, et al. Photovoltaic effect and tribovoltaic effect at liquid-semiconductor interface[J]. **Nano Energy**, 2021, 83: 105810.

[5] Lu Y, Yan Y, Yu X, et al. Polarized water driven dynamic PN junction-based direct-current generator[J]. **Research**, 2021, 2021.

Supporting Figures:

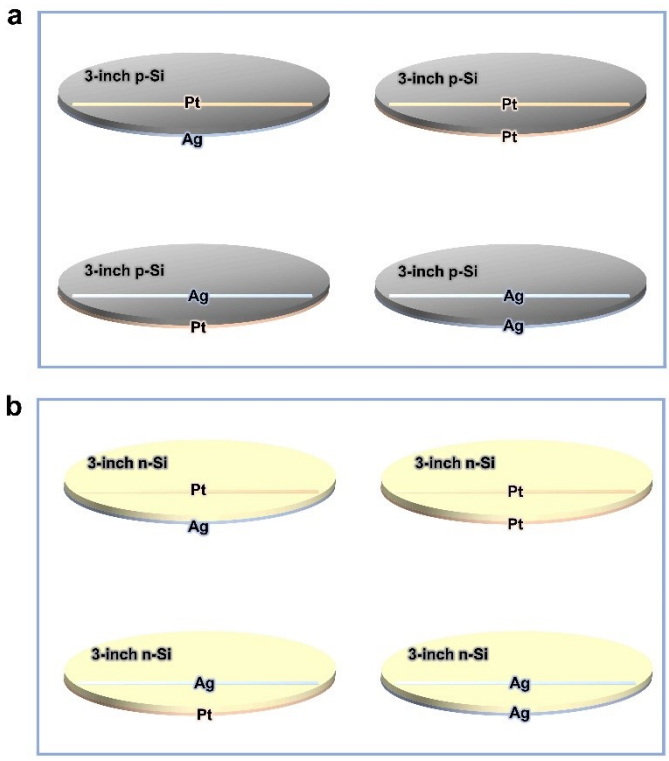

Figure S1. (a) p-Si based MSMs with the asymmetric top and bottom electrodes. (b) n-Si based MSMs with the asymmetric top and bottom electrodes.

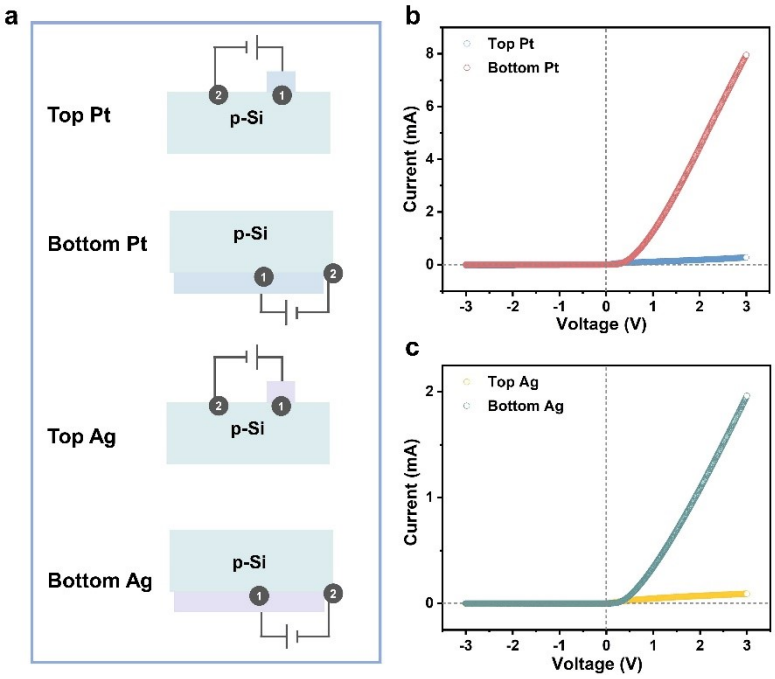

Figure S2. (a) Schematic of the measurement using probe contact. (b) I-V curves of the Schottky contacts formed between Pt and p-Si. (c) I-V curves of the Schottky contacts formed between Ag and p-Si. Note: the contact between tip and p-Si is dominant owing to the higher Schottky barrier.

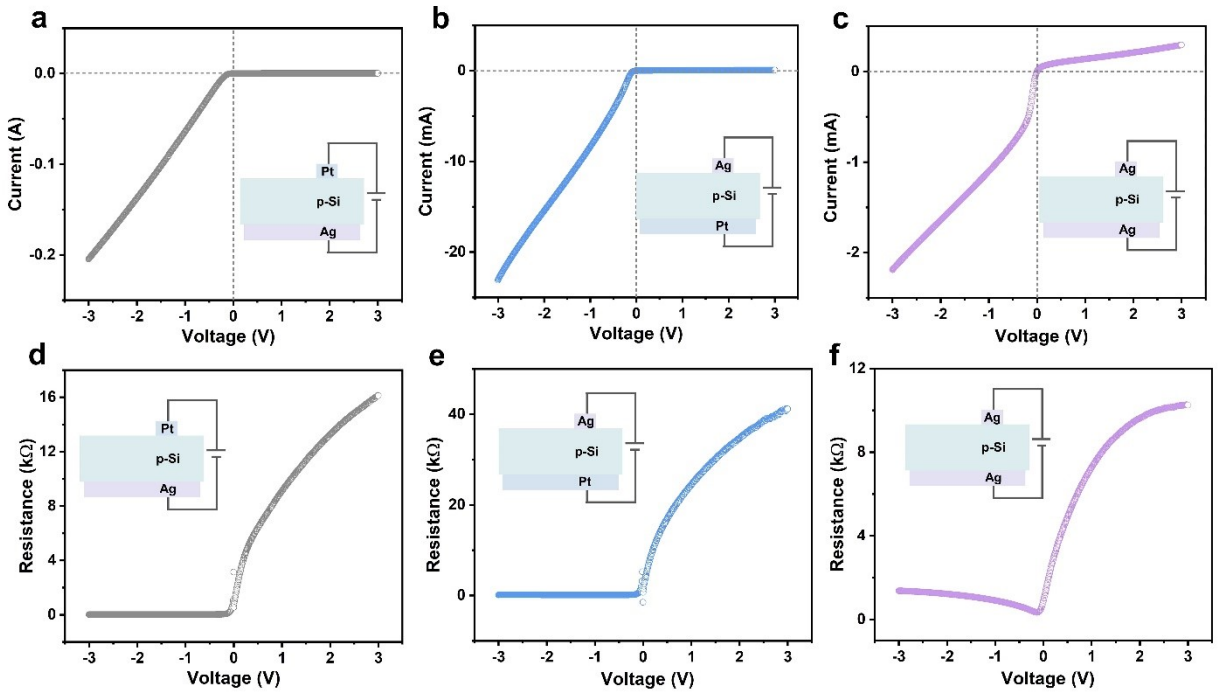

Figure S3. (a-c) I-V curves of the top Pt/bottom Ag, top Ag/bottom Pt, and top Ag/bottom Ag designed MSMs, displaying Schottky character. (d-f) R-V curves of the top Pt/bottom Ag, top Ag/bottom Pt, and top Ag/bottom Ag designed MSMs, displaying Schottky character.

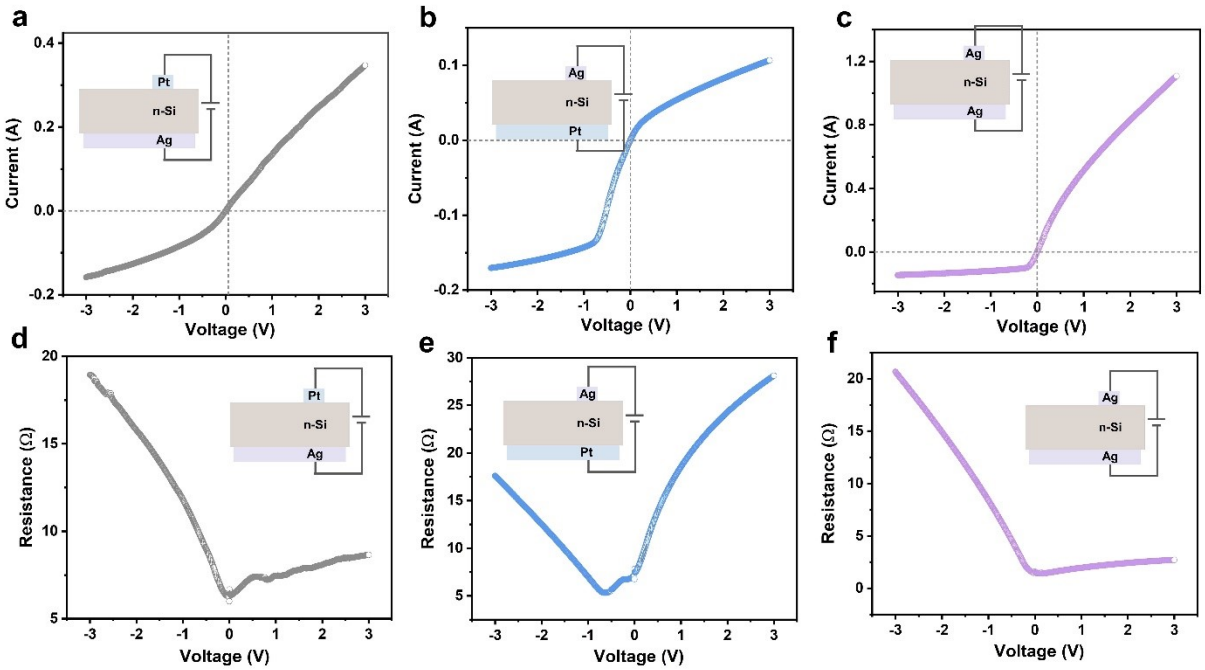

Figure S4. (a-c) I-V curves of the top Pt/bottom Ag, top Ag/bottom Pt, and top Ag/bottom Ag designed MSMs, displaying ohmic-like character. (d-f) R-V curves of the top Pt/bottom Ag, top Ag/bottom Pt, and top Ag/bottom Ag designed MSMs, displaying ohmic-like character.

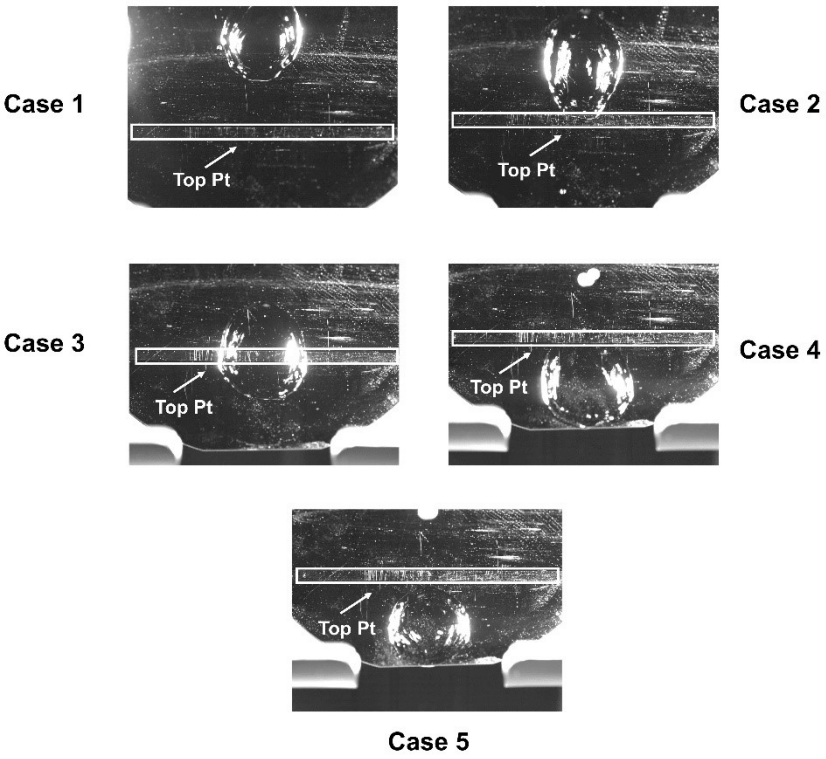

Figure S5. Captured photographs when water droplet impinges onto Si surface. Cases 1 to 5 are the five relative positions between the fully spread water droplet and top electrode.

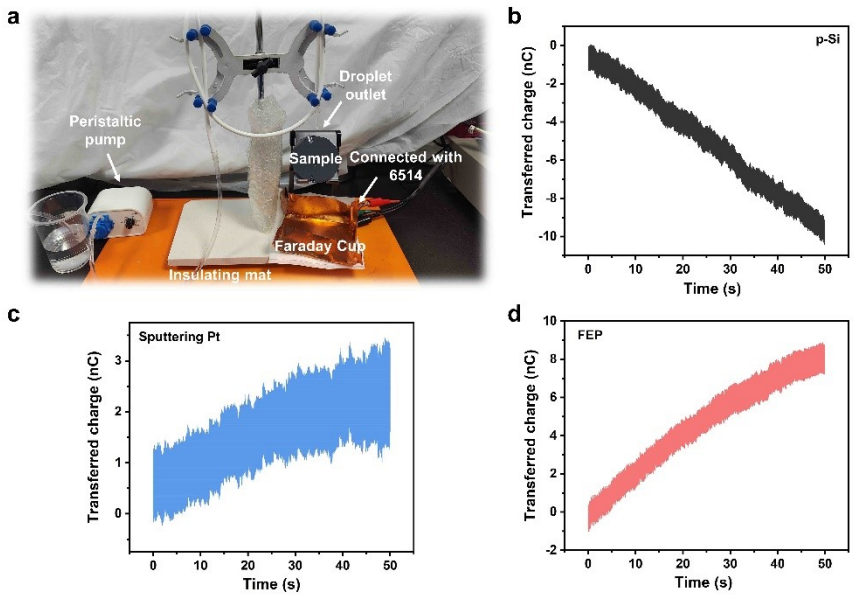

Figure S6. (a) Schematic diagram of the Faraday pail measurement. (b) The measured negative charges carried by water droplet after contacting with p-Si. (c) The measured positive charges carried by water droplet after contacting with Pt. (d) The measured positive charges carried by water droplet after contacting with FEP, which is as a calibrated result due to its well-known strong electron-obtaining capability.

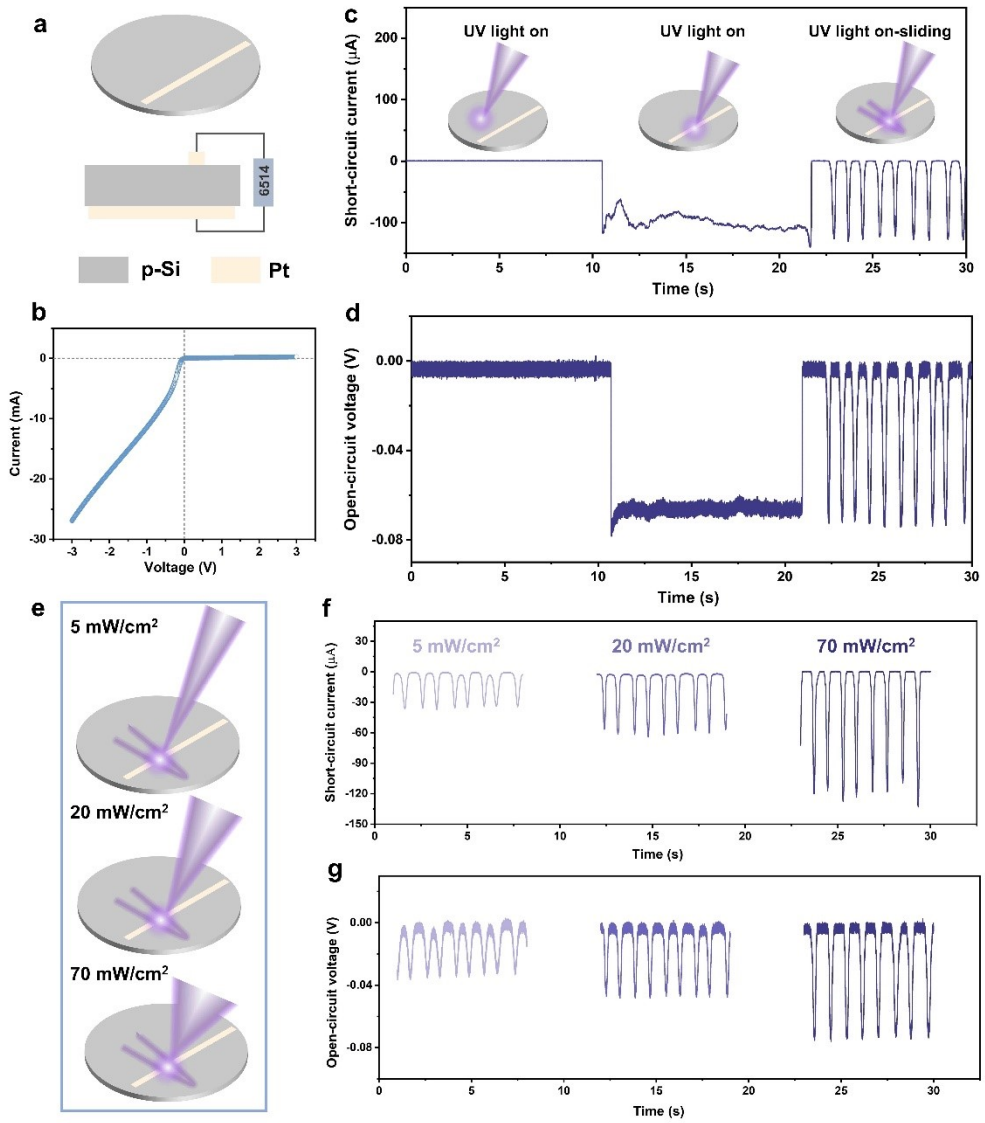

Figure S7. (a) Schematic of MSM based on top Pt/bottom Pt design with the p-Si (1-10 Ω·cm) as contact semiconductor. (b) I-V curve of the top Pt/bottom Pt designed MSM, displaying strict Schottky character. (c,d) Short-circuit current and open-circuit voltage excited by different UV modes with the fixed light intensity of 70 mW/cm^2. The three excitation modes are as the following: illuminate p-Si only, illuminate p-Si and top Pt simultaneously, slide the p-Si and top Pt in turn. (e) Schematic of the MSM driven by sliding mode, and the used light intensity are 5 mW/cm^2, 20 mW/cm^2, and 70 mW/cm^2, respectively. (f,g) Short-circuit current and open-circuit voltage of MSM excited by sliding mode, the output is significantly enhanced as the increasing UV intensity.

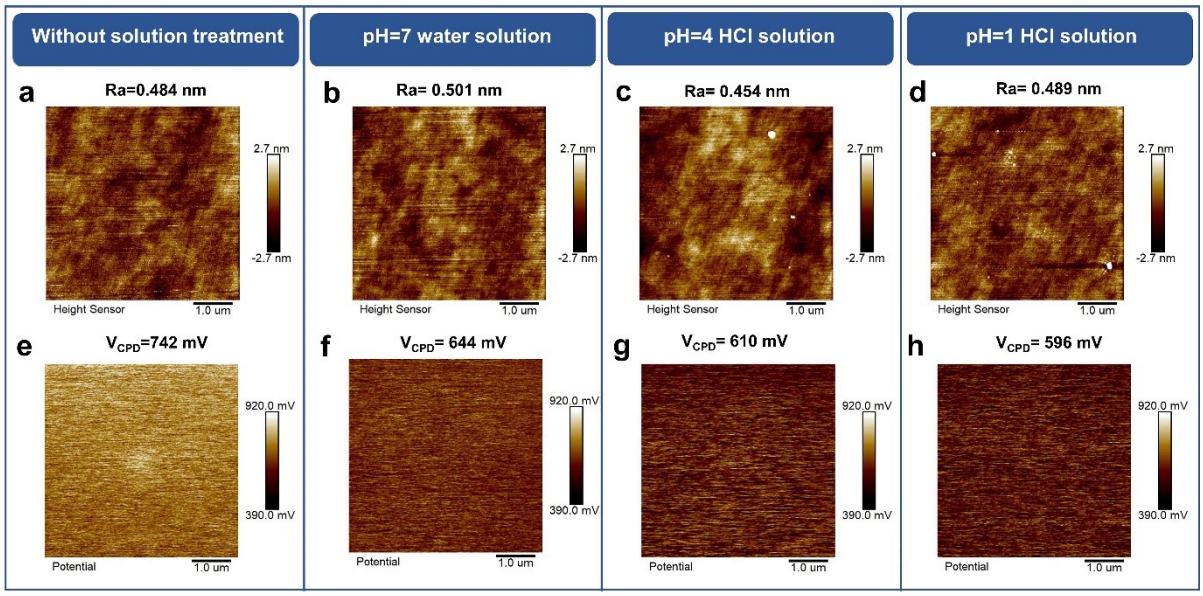

Figure S8. (a-d) The average roughness of p-Si without and with different solutions (water solution and acid solution) impinging. (e-h) The V_{CPD} of p-Si without and with different solutions (water solution and acid solution) impinging.

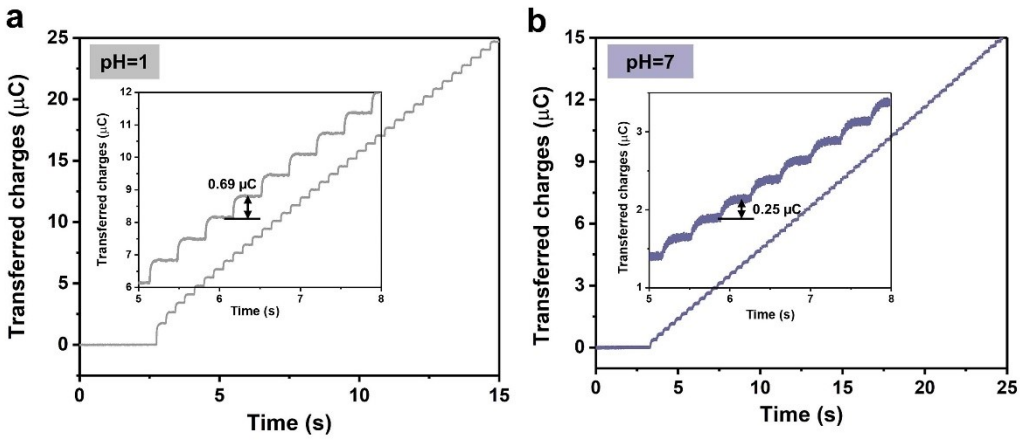

Figure S9. (a) Hydrochloric acid solution with pH equal to 1. (b) Deionized water with pH equal to 7.

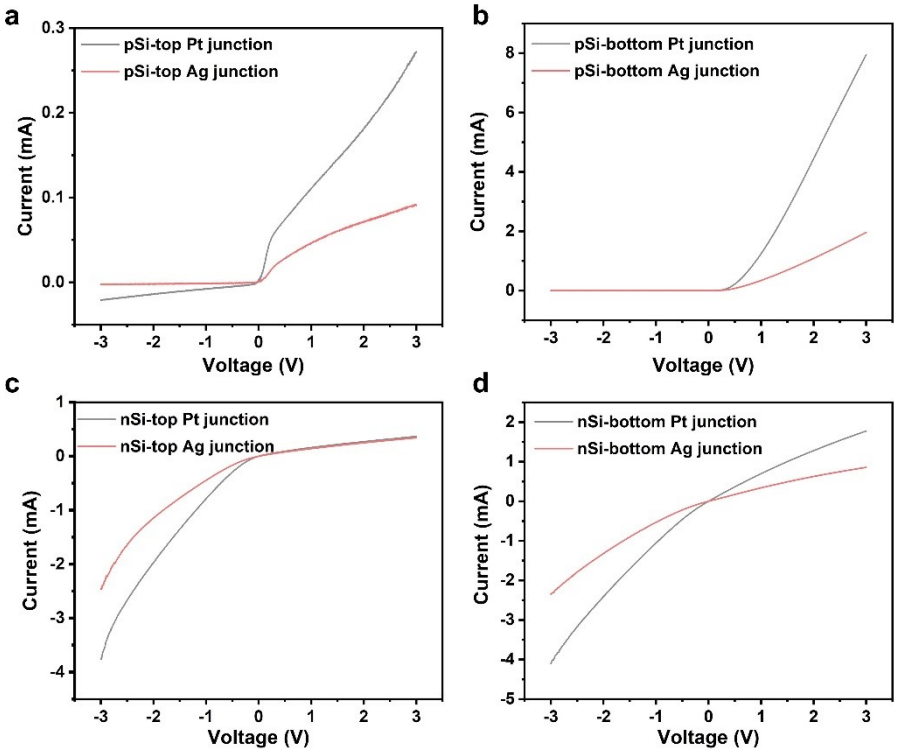

Figure S10. (a) Comparison of Schottky contacts formed by top Pt, top Ag with p-Si. (b) Comparison of Schottky contacts formed by bottom Pt, bottom Ag with p-Si. (c) Comparison of ohmic-like contacts formed by top Pt, top Ag with n-Si. (d) Comparison of ohmic-like contacts formed by bottom Pt, bottom Ag with n-Si.

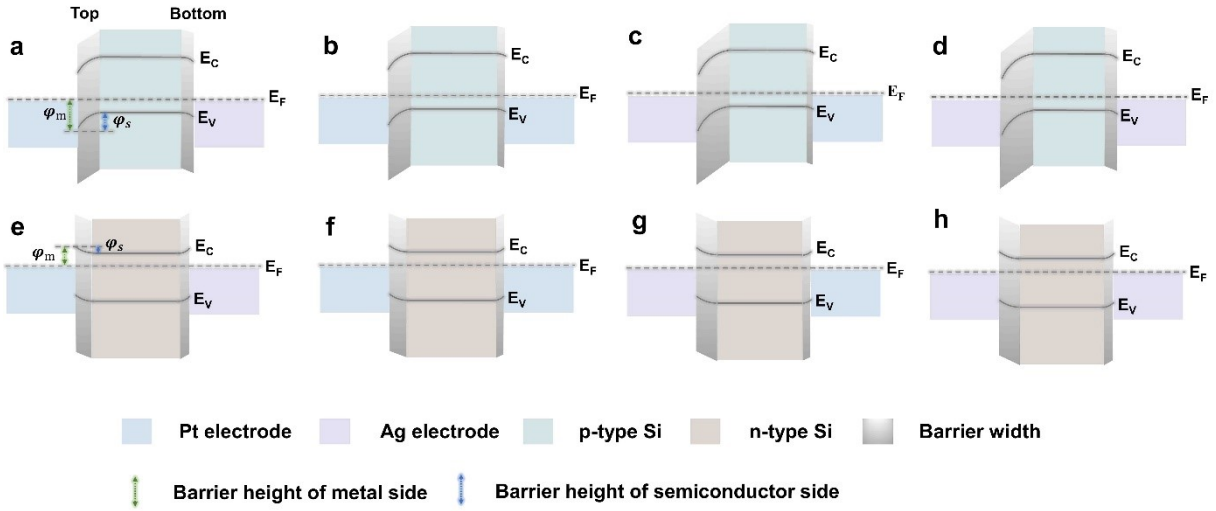

Figure S11. (a-d) Band diagram of p-Si based MSM at thermal equilibrium, showing the top and bottom barriers are asymmetrical. (e-h) Band diagram of n-Si based MSM at thermal equilibrium, showing the top and bottom barriers are asymmetrical.

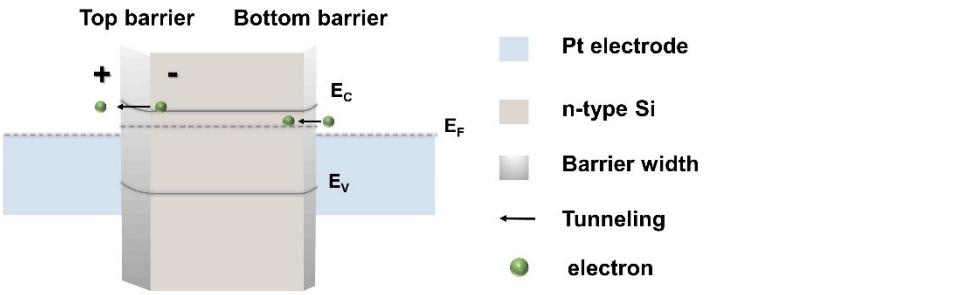

Figure S12. Schematic of water droplet driven ohmic-like n-Si based MSM. The carriers can tunnel through barriers directly with weak bias voltage.

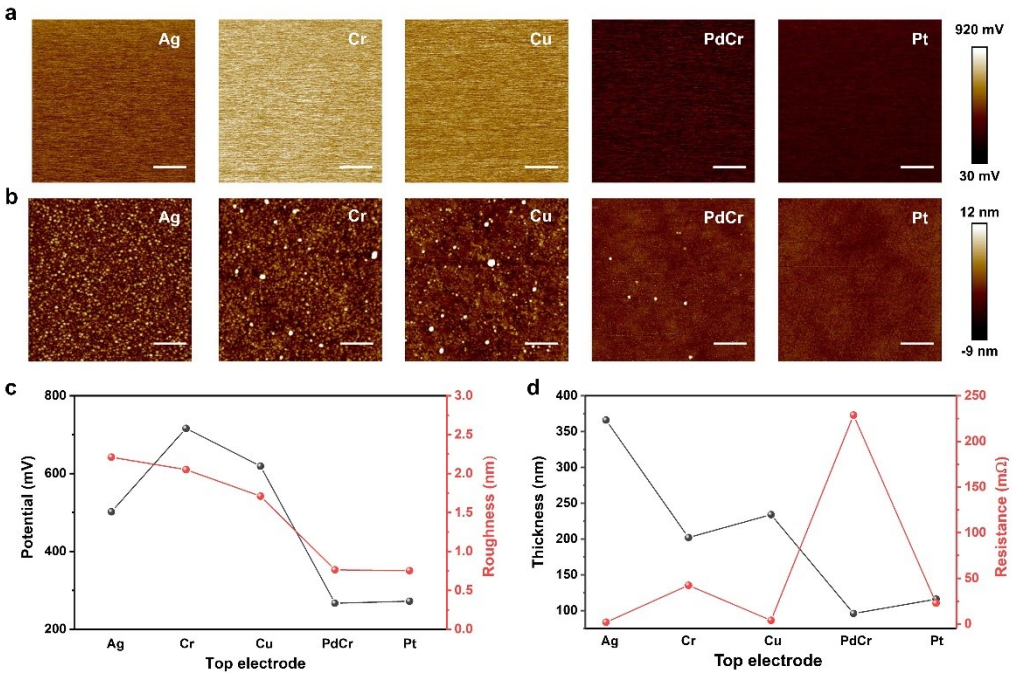

Figure S13. (a) Surface potential distribution images of different metal electrodes. (b) Morphological images of different sputtered electrodes. (c) The comparison of contact potential difference (V_{cpd}) and average roughness of different metal electrodes. (d) The comparison of thickness and resistance of different sputtered electrodes.

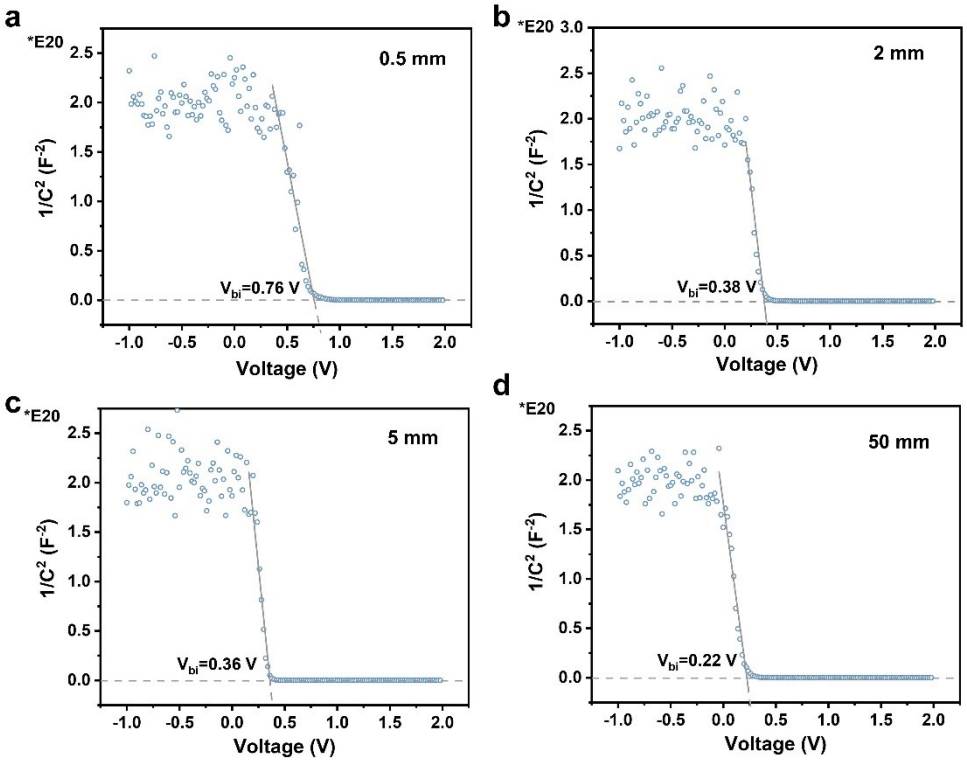

Figure S14. Schottky-Mott characteristics of the p-Si/Pt contacts. $1/C^2$-V curves of the Schottky contacts formed between various width top Pt and p-Si, the calculated built-in voltage is 0.76 V, 0.38 V, 0.36 V, and 0.22 V, respectively.

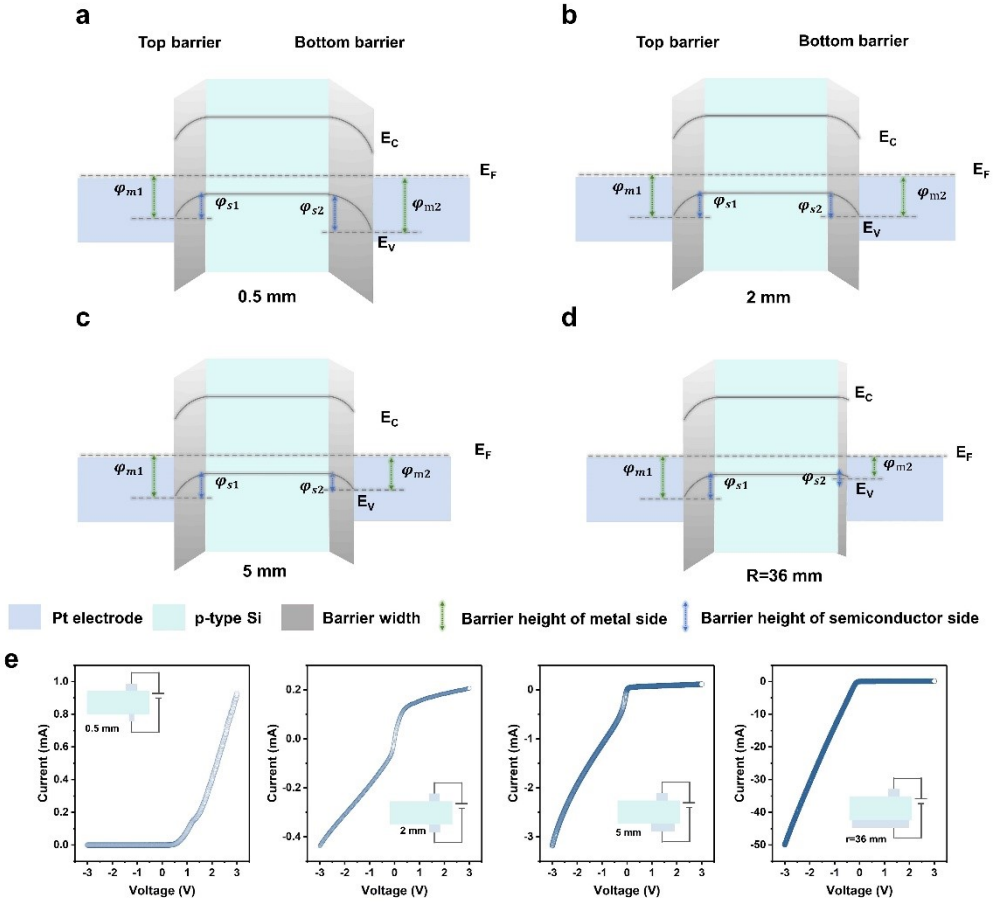

Figure S15. (a-d) Band diagrams of p-Si based MSM with different bottom electrode structures, the barrier thickness decreases with the increasing electrode area. (e) I-V curves of p-Si based MSM with different bottom electrode designs, where the top barrier is Schottky character.

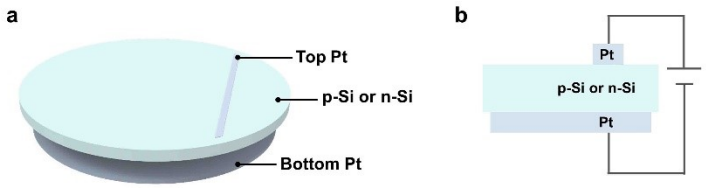

Figure S16. (a) Schematic diagram of MSM, where the electrode material and structure are as the same. (b) Side view of the I-V measurement.

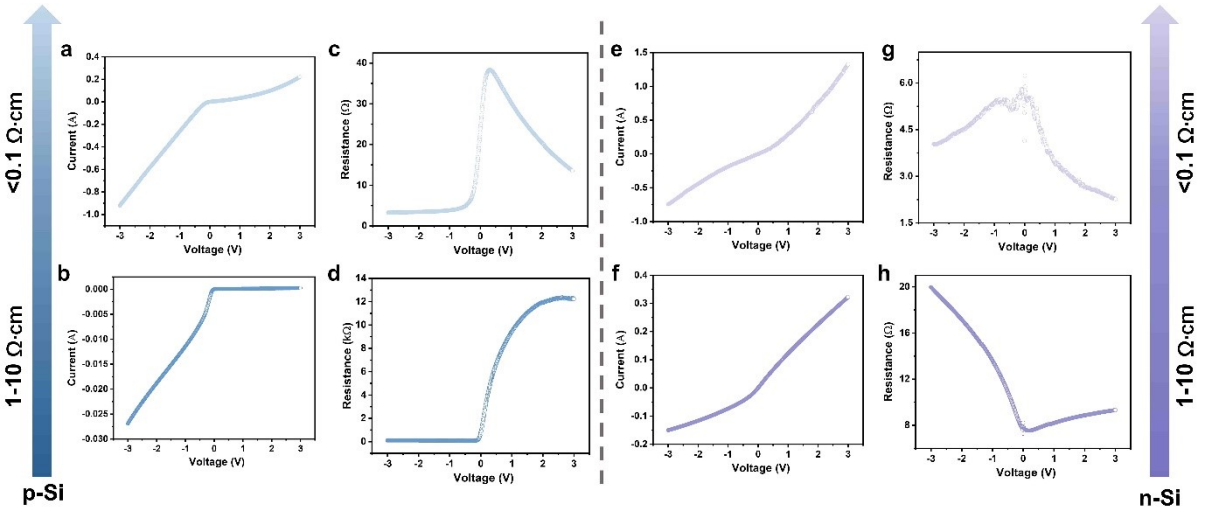

Figure S17. (a-d) I-V and R-V curves of p-Si based MSMs, the contact character is changed from ohmic type to Schottky contact as the as the resistivity increases. (e-h) I-V and R-V curves of n-Si based MSMs, showing ohmic type, and the internal resistance of MSM increases as the increasing resistivity.

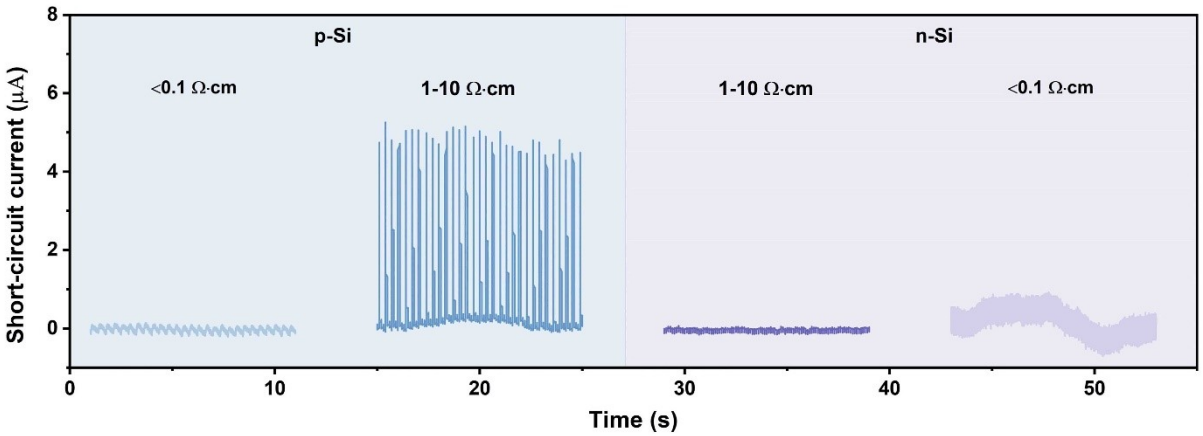

Figure S18. Output based on different semiconductor MSM driven by water droplet. Schottky MSMs can generate electricity, and ohmic-like MSM do not respond to the water droplet excitation.

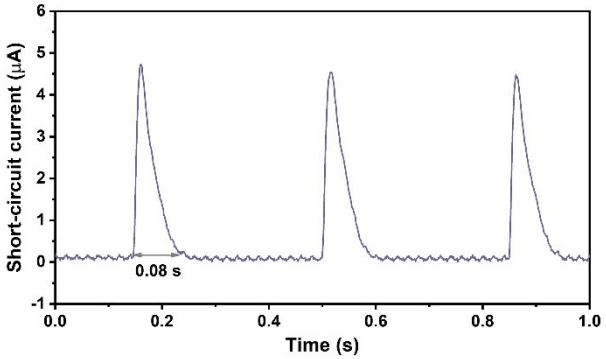

Figure S19. The output details of Schottky MSM driven by single water droplet. The duration of Schottky barrier under the routine excitation in this work is about 0.08 s.

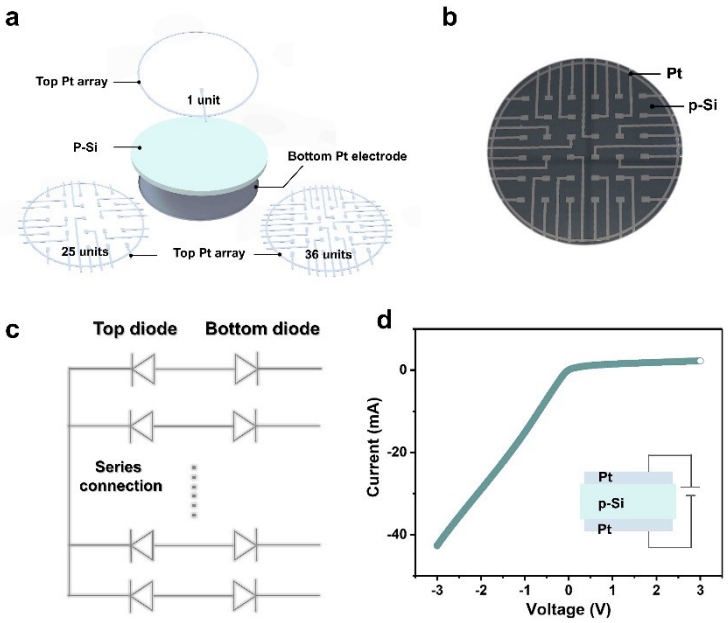

Figure S20. (a) The designed MSMs with different top Schottky diode arrays, where the bottom M-S junction is ohmic character. (b) The photography of fabricated MSM with 36 array channels. (c) The equivalent circuit of Schottky diode arrays based on MSM structure, in which the top diodes are in series and share the bottom diode. (d) The I-V curve of MSM with 36 array channels as the top Schottky barrier regions.

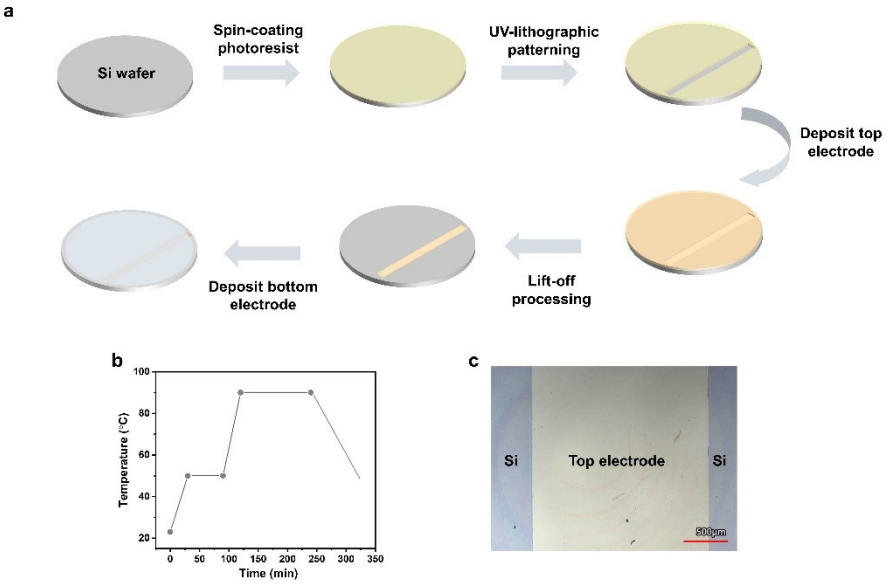

Figure S21. (a) Manufacturing process of MSM, mainly involves spin coating, curing, lithography patterning, sputtering, lift-off and other processes. (b) Temperature program of AZ4620 photoresist during curing process. (c) Optical microscope image of the top electrode, showing the electrode structure is complete without damage.

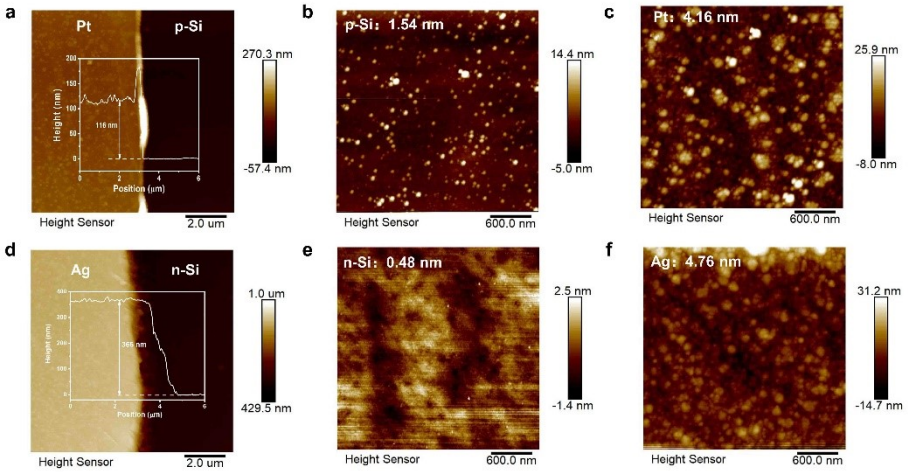

Figure S22. (a) Height difference between p-Si and Pt, indicating the thickness of sputtered Pt is about 116 nm. (b,c) AFM images of polished p-Si and Pt, showing the average roughness of p-Si and Pt is 1.54 nm and 4.16 nm. (d) Height difference between n-Si and Ag, indicating the thickness of sputtered Ag is about 366 nm. (e,f) AFM images of polished n-Si and Ag, showing the average roughness of n-Si and Ag is 0.48 nm and 4.76 nm.

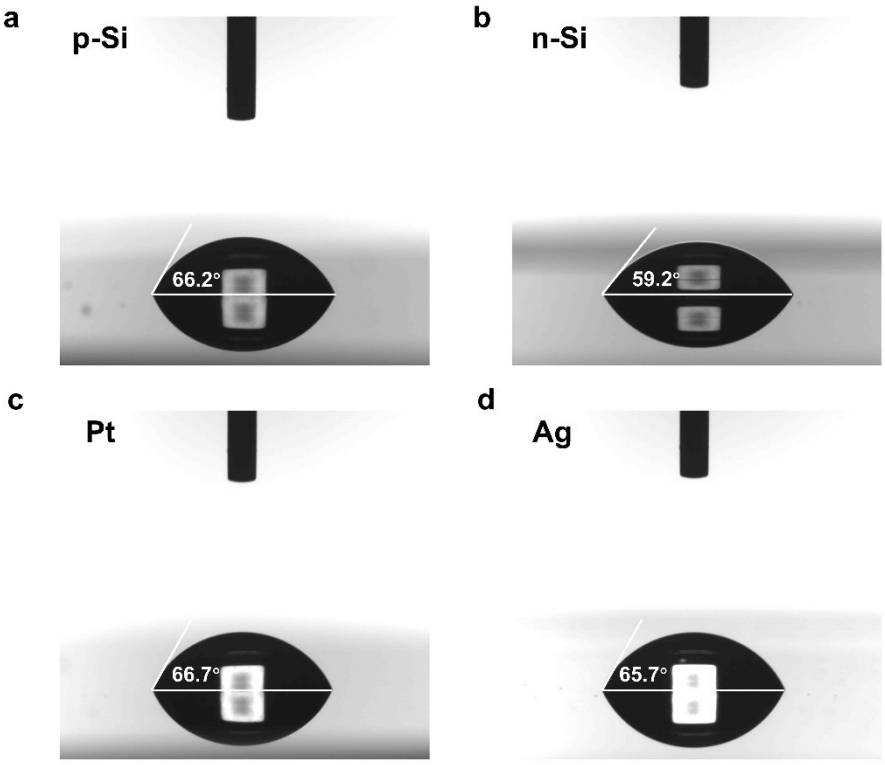

Figure S23. (a-d) The static contact angles for polished p-Si, polished n-Si, Pt, and Ag, which are 66.2°, 59.2°, 66.7°, and 65.7°, respectively. The static contact angles are less than 90° without excellent hydrophobic performance.

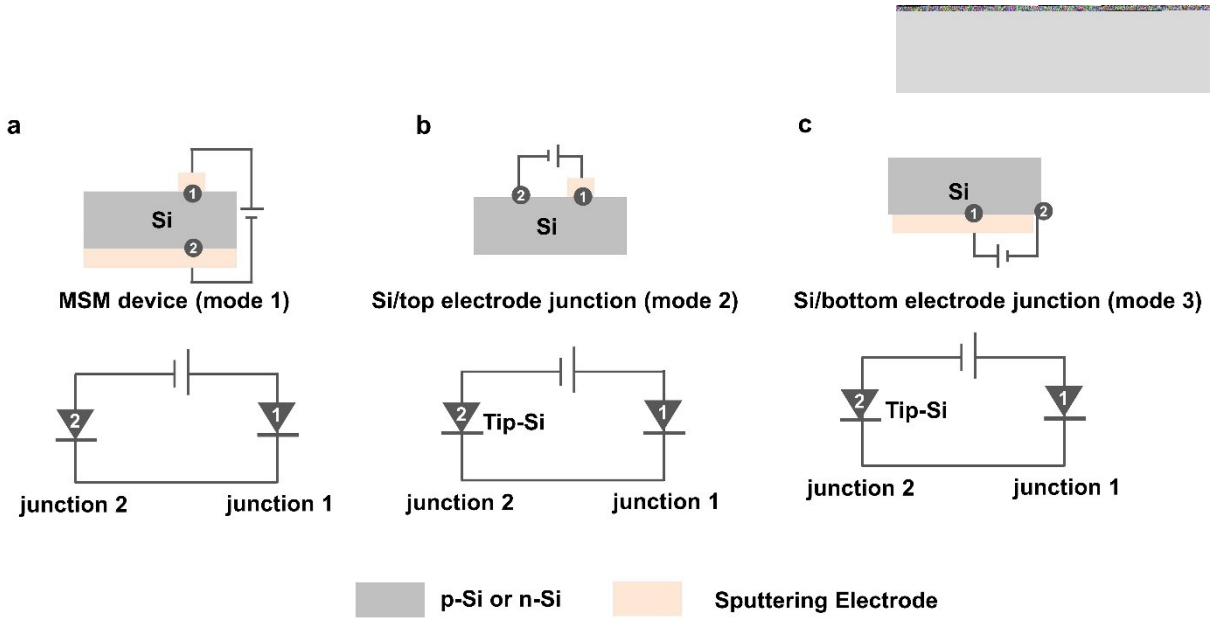

Figure S24. (a) Side view of the measurement schematic on MSM device, the top electrode is connected to positive electrode and bottom electrode is connected to negative electrode. (b,c) Side view of the measurement schematic on metal-semiconductor contact, the electrode is connected to positive electrode and Si is connected to negative electrode with contacting probe.

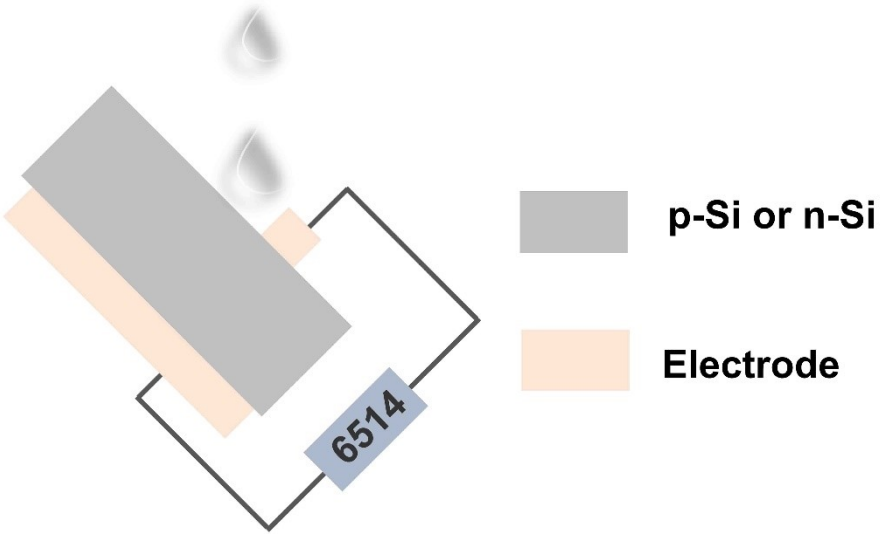

Figure S25. Side view of the measurement setup for water droplet excitation on MSM device, the droplets are continuously produced by a kcp-c peristaltic pump.